12th Int. Particle Acc. Conf. IPAC2021, Campinas, SP, Brazil JACoW Publishing
ISBN: 978-3-95450-214-1 ISSN: 2673-5490 doi:10.18429/JACoW-IPAC2021-TUPAB077

NOVEL OPEN CAVITY FOR ROTATING MODE SLED-TYPE RF PULSE COMPRESSORS

Xiaowei Wu*, Alexej Grudiev
European Organization for Nuclear Research (CERN), Geneva, Switzerland

Abstract

A new X-band high-power rotating mode SLAC Energy Doubler (SLED)-type rf pulse compressor is proposed. It is based on a novel cavity type, a single open bowl-shape energy storage cavity with high Q_0 and compact size, which is coupled to the waveguide using a compact rotating mode launcher. The novel cavity type is applied to the rf pulse compression system of the main linac rf module of the klystron-based option of the Compact Linear Collider (CLIC). Quasi-spherical rotating modes of $TE_{1,2,4}$ and $TE_{1,2,13}$ are proposed for the correction cavity and storage cavity of the rf pulse compression system respectively. The storage cavity working at $TE_{1,2,13}$ has a Q_0 of 240000 and a diameter less than 33 cm. The design of the pulse compressor and in particular of the high-Q cavity will be presented in detail.

INTRODUCTION

As an alternative to the original two beam Compact Linear Collider (CLIC) concept, the klystron-based CLIC option is considered for the 380 GeV initial energy stage [1]. An X-band rf pulse compressor with correction cavities was selected as a base line option for the klystron-based CLIC rf module [2–4]. RF compression obtains high peak power in exchange for reduced rf pulse length. The first rf pulse compressor named SLAC Energy Doubler (SLED) was invented in 1974 [5]. The key components of a SLED system include a 3 dB coupler with two 90° apart divided power ports and two high-Q energy storage cavities. Different resonant cavities such as barrel open cavity (BOC), single spherical cavity, and corrugated circular cavity were designed in the past years [6–8].

The parameters of the CLIC accelerating structure had been re-evaluated to improve the accelerator performance [9]. Additionally, the pulse compressor design adopted to the new structure parameters was optimized based on the klystron output [10]. It is suggested that a correction cavity with a Q_0 of 6×10^4 and a storage cavity with a Q_0 of 2.4×10^5 is a good compromise that increases the power gain by 7.5% compared to the initial design: from 3.48 to 3.74. A novel compact open bowl-shape energy storage cavity with high Q_0 is proposed to meet the requirements for both the correction cavity and storage cavity of CLIC. This novel cavity type with rotating mode could also be applied to other pulse compression systems. This paper describes its principle, design, and technical advances.

* xiaowei.wu@cern.ch

CAVITY DESIGN

The novel open cavity has a bowl shape, as shown in Fig. 1. It works in a quasi-spherical rotating mode of $TE_{1,2,i}$ which is a dipole mode. The radial index i is dominated by R_{cav}. The working mode shown in Fig. 1 is $TE_{1,2,13}$. The Q_0 of $TE_{1,2,13}$ at 12 GHz is around 2.4×10^5. Principally, the larger R_{cav} contributes to a higher radial index which results in a higher quality factor. However, more parasitic modes will appear in a larger cavity. The parasitic modes may have high field on the top area which results in high loss in the open boundary. The coupling from parasitic modes to working modes will impact the performance of the pulse compressor. The frequency separation between working mode and parasitic modes should be kept as large as possible. Otherwise absorption materials such as silicon carbide need to be added to damp such modes. DZ_{cav} and R_{arc} are used to optimize the Q_0 of the working mode and the mode separation between working mode and parasitic modes.

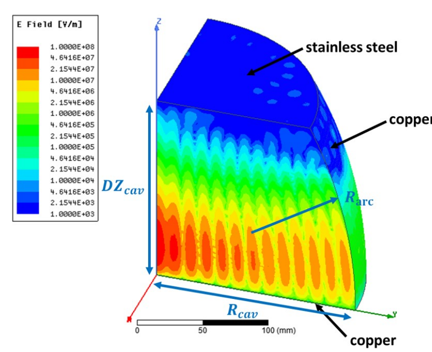

Figure 1: Electrical field of the bowl-shape open cavity operating at $TE_{1,2,13}$ at 12 GHz. The electrical field is in logarithmic scale.

The electrical field of the working mode in the top area of the cavity is very small. Thus the top of the cavity can be kept open. The open boundary will also help us to suppress many parasitic modes. The cavity can be easily machined by lathe due to its symmetric and open shape. No brazing is needed for the cavity manufacture. This can reduce the cost of the fabrication and increases the fabrication accuracy. The top of the cavity is connected to the stainless steel flange with pumping port. This will make it easier to pump compared with the spherical pulse compressor.

CORRECTION CAVITY DESIGN

The Q_0 of the correction cavity is suggested to be 6×10^4 from Ref. [10]. $TE_{1,2,4}$ mode is selected for the bowl-shaped

ISBN: 978-3-95450-214-1 ISSN: 2673-5490 doi:10.18429/JACoW-IPAC2021-TUPAB077

open cavity design with the R_{cav} around 50 mm. The Q_0 is around 75000. As mentioned in the previous chapter, coupling to the parasitic modes is one of the critical issues in the design. A single cavity model with stainless steel boundary on the top is created to calculate the quality factor (Q_{ss}) and the mode frequency separation. The mode spectrum for different R_{arc} is shown in Fig. 2. The middle line with high Q_{ss} is the working mode of $TE_{1,2,4}$ while the other lower Q_{ss} points are the parasitic modes. R_{arc}=300 mm is selected for the correction cavity design as it has large mode separation from the nearest two parasitic modes with high Q_{ss} value.

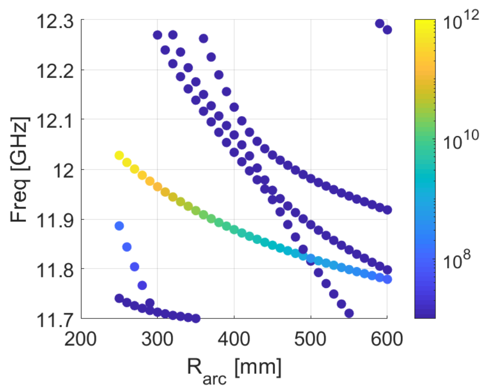

Figure 2: Mode spectrum of $TE_{1,2,4}$ mode cavity. DZ_{cav} is 95 mm. R_{cav} is 49.2 mm. Color bar presents the value of Q_{ss}.

Though the optimized cavity shape has a large frequency separation between working mode and parasitic modes, the coupling to the parasitic modes may still increase the field at the open area of the cavity. Therefore, the loss in the open boundary area needs to be checked. The top of the cavity model with coupling iris and circular waveguide is set to stainless steel boundary. TE_{11} rotating mode propagates in the circular waveguide and excites $TE_{1,2,4}$ mode in the open cavity via the coupling iris. A quantity named *lossratio* is defined as the ratio between the loss in the stainless steel and in the copper of the model. The coupling iris is optimized to get the required Q_{ext} and minimum *lossratio*. The minimum *lossratio* of 0.6% is obtained when the coupling iris radius is 4.10 mm.

The frequency and quality factor of the working mode and the nearest two parasitic modes are summarized in Table 1. The two parasitic modes are around 250 MHz and 300 MHz away from the working frequency respectively.

Table 1: Modes of the Correction Cavity

	Frequency [GHz]	Q_0
Working mode	12.001	74648.9
Parasitic mode1	11.7523	16449.1
Parasitic mode2	12.3093	14989.6

The electrical field of the working mode and the parasitic modes are shown in Fig. 3.

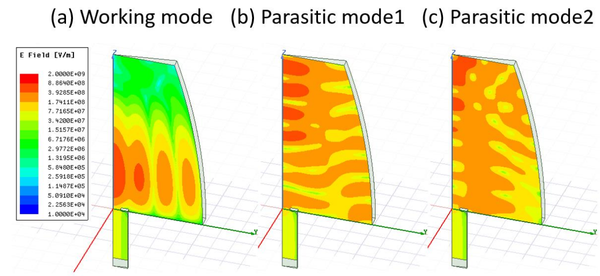

Figure 3: Electrical field of the working mode and parasitic modes in the correction cavity. The electrical field is in logarithmic scale. (a) is the working mode at 12 GHz. (b) and (c) are the parasitic modes.

The so-called E-rotator is used as 3 dB coupler for the SLED system of the bowl-shape open cavity. It is an rf device with two rectangular and one circular waveguide ports, as shown in Fig. 4. If the input signal comes to the rectangular port 1, the output mode is a right-circularly-polarized TE_{11} mode, as shown in Fig. 4 (left). If the input signal comes to port 2, a left-circularly-polarized TE_{11} mode is formed, as shown in Fig. 4 (right) [11]. A similar device with the same functionality but different design concept, an rf polarizer, is described in Ref. [12].

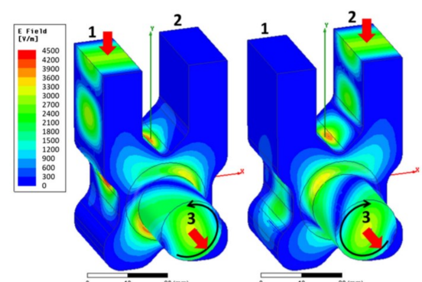

Figure 4: E-rotator geometry and electric field distribution for 1 W of input power into port 1 (left) and port 2 (right). The polarization of the circular TE_{11} mode in the output port is indicated using black arrows [12].

The S_{12} frequency sweep of the correction cavity system is shown in Fig. 5. The electrical field distribution is shown in Fig. 6.

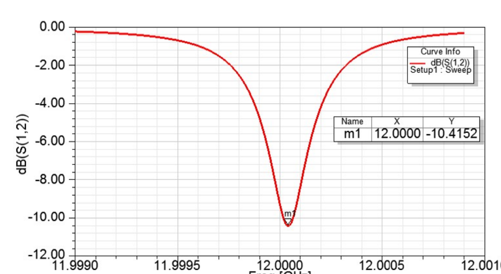

Figure 5: Frequency sweep showing the working mode $TE_{1,2,4}$.

ISBN: 978-3-95450-214-1 ISSN: 2673-5490 doi:10.18429/JACoW-IPAC2021-TUPAB077

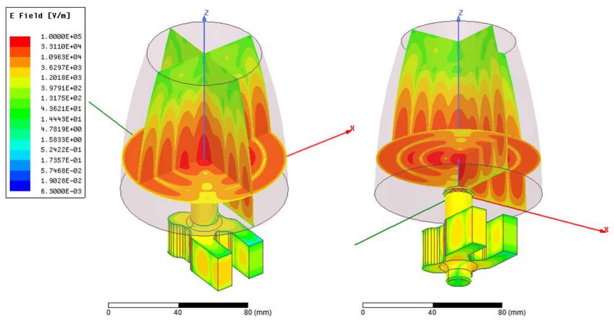

Figure 6: Electrical field distribution of the correction cavity with the E-rotator. The electrical field is in logarithmic scale.

STORAGE CAVITY DESIGN

The Q_0 of the storage cavity is suggested to be 2.4×10^5 from Ref. [10]. $TE_{1,2,13}$ mode is selected for the bowl-shaped open cavity design with R_{cav} around 165 mm. The Q_0 is around 240000. The mode spectrum of the storage cavity for different R_{arc} is shown in Fig. 7. The middle line with high Q_{ss} is the working mode of $TE_{1,2,13}$ while the other lower Q_{ss} points are the parasitic modes. R_{arc}=360 mm is selected for the storage cavity design as it has a high Q_{ss} value and a large mode separation from the nearest two parasitic modes.

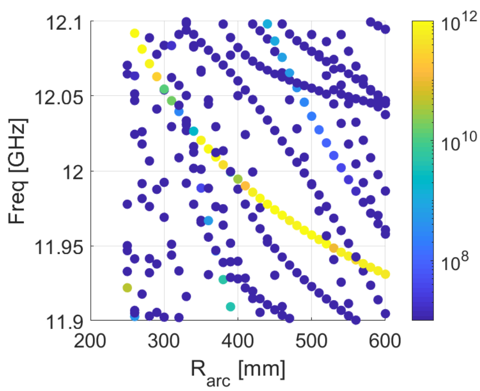

Figure 7: Mode spectrum of $TE_{1,2,13}$ mode cavity. DZ_{cav} is 160.2 mm. R_{cav} is 163.6 mm. Color bar presents the value of Q_{ss}.

As with the design of the correction cavity, the loss in the open boundary area is checked. The minimum *lossratio* of 0.7% is obtained when the coupling iris radius is 4.903 mm. However, the frequency separation between working mode and parasitic modes is smaller than that of the correction cavity, as shown in Table 2. The three parasitic modes are around 26 MHz, 30 MHz, and 33 MHz away from the working frequency respectively.

The electrical field of the working mode and the parasitic modes are shown in Fig. 8. Compared with the $TE_{1,2,4}$ mode of the correction cavity, the $TE_{1,2,13}$ mode has smaller mode separation which may cause instability during operation. A ring-shape silicon carbide attached to the top of the cavity is being designed to suppress the parasitic modes. Additionally, a lower-order mode of $TE_{1,2,12}$ is also being considered for the storage cavity design to get larger mode separation between working mode and parasitic modes. The studies of silicon carbide optimization and $TE_{1,2,12}$ mode cavity are in progress.

Table 2: Modes of the Storage Cavity

	Frequency [GHz]	Q_0
Working mode	11.9999	240097
Parasitic mode1	11.9738	63916.8
Parasitic mode2	12.0298	25837.1
Parasitic mode2	12.0327	61996.2

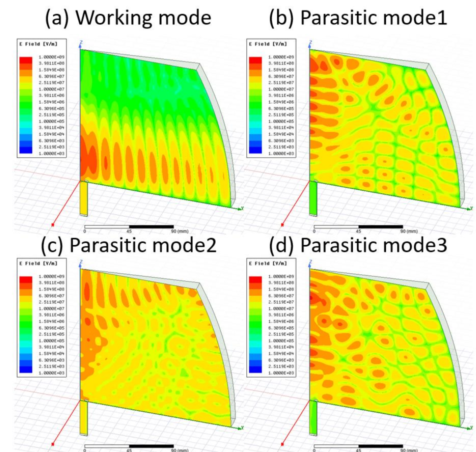

Figure 8: Electrical field of the working mode and parasitic modes in the storage cavity. The electrical field is in logarithmic scale. (a) is the working mode at 12 GHz. (b), (c) and (d) are the parasitic modes.

CONCLUSION

A new X-band high-power rotating mode SLED-type rf pulse compressor is proposed. It is based on a single open bowl-shape energy storage cavity working at quasi-spherical rotating mode. It has high Q_0 and compact size. The cavity is coupled to a circular waveguide with a compact rotating mode launcher. An open cavity working at $TE_{1,2,4}$ mode is proposed for the correction cavity design of CLIC rf pulse compression system. Preliminary design for storage caivty of CLIC based on $TE_{1,2,13}$ mode indicates high Q_0 and compact size. However, the mode separation between working mode and parasitic modes is around 30 MHz. Further optimization and study are still in progress.

REFERENCES

[1] M. Aicheler *et al.*, *The Compact Linear Collider (CLIC) – Project Implementation Plan*, Geneva, Switzerland: CERN Yellow Reports: Monographs. Mar. 2019.

[2] S. Y. Kazakov, "Pulse Shape Correction for RF Pulse Compression System", in *Proc. 3rd European Particle Accelerator*

ISBN: 978-3-95450-214-1 ISSN: 2673-5490 doi:10.18429/JACoW-IPAC2021-TUPAB077

Conf. (EPAC'92), Berlin, Germany, Mar. 1992, pp. 1247-1249.

[3] P. Wang, H. Zha, I. Syratchev, J. Shi, and H. Chen, "Rf design of a pulse compressor with correction cavity chain for klystron-based compact linear collider", *Phys. Rev. Accel. Beams*, vol. 20, p. 112001, Nov. 2017. doi:10.1103/PhysRevAccelBeams.20.112001

[4] Y. Jiang *et al.*, "Demonstration of a cavity-based pulse compression system for pulse shape correction", *Phys. Rev. Accel. Beams*, vol. 22, p. 082 001, 8 Aug. 2019. doi:10.1103/PhysRevAccelBeams.22.082001

[5] Z. D. Farkas, H. A. Hoag, G. A. Loew, and P. B. Wilson, "SLED: A Method of Doubling SLAC's Energy", in *Proc. 9th Int. Conf. on High-Energy Accelerators*, Stanford, CA, USA, May 1974, pp. 576–583.

[6] I. V. Syrachev, "The Progress of X-Ban "Open" Cavity RF Pulse Compression Systems", in *Proc. 4th European Particle Accelerator Conf. (EPAC'94)*, London, UK, Jun.-Jul. 1994, pp. 375-380.

[7] J. W. Wang *et al.*, "Development for a supercompact -band pulse compression system and its application at slac", *Phys. Rev. Accel. Beams*, vol. 20, p. 110401, Nov. 2017. doi:10.1103/PhysRevAccelBeams.20.110401

[8] Y. L. Jiang *et al.*, "The X-Band Pulse Compressor for Tsinghua Thomson Scattering X-Ray Source", in *Proc. 8th Int. Particle Accelerator Conf. (IPAC'17)*, Copenhagen, Denmark, May 2017, pp. 4214-4217. doi:10.18429/JACoW-IPAC2017-THPIK054

[9] J. Liu and A. Grudiev, "RF design of accelerating structure for the main linac of the klystron-based first stage of CLIC at 380 GeV", CERN, Geneva, Switzerland, Rep. CERN-ACC-2018-0034, Oct. 2018.

[10] J. Cai and I. Syratchev, "The design update of the X-band RF pulse compressor with Correction Cavities for the CLIC 380 GeV klystron based accelerator", CERN, Geneva, Switzerland, Rep. CERN-ACC-2020-0031, Oct. 2020.

[11] A. Grudiev, "design of compact high power rf components at x-band", CERN, Geneva, Switzerland, Rep. CERN-ACC-NOTE-2016-0044, May 2016.

[12] M. Franzi, J. Wang, V. Dolgashev, and S. Tantawi, "Compact rf polarizer and its application to pulse compression systems", *Phys. Rev. Accel. Beams*, vol. 19, p. 062002, Jun. 2016. doi:10.1103/PhysRevAccelBeams.19.062002